

Article

Viscoelastic Properties of Crosslinked Chitosan Films

Joseph Khouri, Alexander Penlidis  and Christine Moresoli *

Department of Chemical Engineering, University of Waterloo, 200 University Avenue West, Waterloo, ON N2L 3G1, Canada; j2khouri@uwaterloo.ca (J.K.); penlidis@uwaterloo.ca (A.P.)

* Correspondence: cmoresoli@uwaterloo.ca; Tel.: +1-519-888-4567 (ext. 35254)

Received: 17 February 2019; Accepted: 8 March 2019; Published: 14 March 2019



Abstract: Chitosan films containing citric acid were prepared using a multi-step process called heterogeneous crosslinking. These films were neutralized first, followed by citric acid addition, and then heat treated at 150 °C/0.5 h in order to potentially induce covalent crosslinking. The viscoelastic storage modulus, E' , and $\tan\delta$ were studied using dynamic mechanical analysis, and compared with neat and neutralized films to elucidate possible crosslinking with citric acid. Films were also prepared with various concentrations of a model crosslinker, glutaraldehyde, both homogeneously and heterogeneously. Based on comparisons of neutralized films with films containing citric acid, and between citric acid films either heat treated or not heat treated, it appeared that the interaction between chitosan and citric acid remained ionic without covalent bond formation. No strong evidence of a glass transition from the $\tan\delta$ plots was observable, with the possible exception of heterogeneously crosslinked glutaraldehyde films at temperatures above 200 °C.

Keywords: chitosan; crosslinking; viscoelasticity; citric acid; glutaraldehyde; heterogeneous crosslinking

1. Introduction

The search for biodegradable and non-toxic materials to offset the consumption and production of plastics for the food industry has led to research on polysaccharide edible films, including chitosan, the crustacean-derived aminopolysaccharide. Chitosan films have been studied either in stand-alone form as potential packaging or wrapping products or as coatings [1]. The physico-chemical properties of films prepared by the solvent casting method have been well studied, including in relation to the organic acids used in film preparation (e.g., acetic, lactic, citric acid, etc.) [2,3], the molecular weight of chitosan [3], and the degree of deacetylation [4,5]. The degree of deacetylation (DD) is the percentage of glucosamine residues with a primary amine side group at the C-2 position. The chemical structure of chitosan is given in Figure 1.

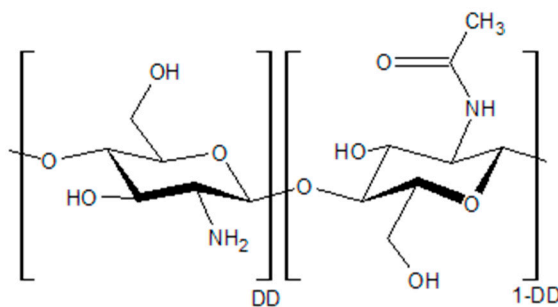


Figure 1. The glucosamine and acetyl glucosamine units that comprise chitosan and chitin. When the degree of deacetylation (DD) is greater than 0.6, the polymer is considered chitosan.

While chitosan films have advantages, such as high anti-microbial and low oxygen-permeability properties [3], their high moisture affinity and relatively poorer mechanical properties compared to common plastics, such as polyethylene terephthalate, low density polyethylene, and polypropylene, limit their packaging applications. The water vapor permeability (WVP) of chitosan films is typically a magnitude higher than that of thermoplastics. Their tensile strength (TS) is in the same range as some plastics; however, their elongation capacities and elastic moduli are lower. A comparison of mechanical and barrier properties of chitosan and plastic films is provided in Table 1.

Improving mechanical properties and reducing hydrophilicity of chitosan films has been attempted by several methods, including (i) composite formation with fatty acids [6,7] and other polysaccharides [8], (ii) grafting hydrophobic compounds [9,10] or phenolics [11,12], and (iii) crosslinking the polymer chains [8]. Composites with hydrophobic compounds, such as beeswax [13], or fatty acids such as stearic [7] and palmitic [13] acid, do not always improve WVP, possibly as a consequence of a decrease in film density [6,13]. Composites with starch [14] and cellulose-derivatives [15] or with proteins such as gelatin [14] have ultimately not shown much improvement in the WVP and TS properties of chitosan films. Crosslinking appears to be a promising method for modification for food-related applications.

Table 1. Properties of Chitosan Films and Plastics from Literature.

Property	Chitosan	Common Plastics
Water Vapor Permeability (WVP) (g/(m·s·Pa))	1–10 × 10 ^{−11} [2,3,6,7,15]	0.01–1 × 10 ^{−11} [16–18]
Oxygen Gas Permeability (OP) (cm ³ /(m·s·Pa))	1 × 10 ^{−15} –1 × 10 ^{−13} [3,6,7,15]	1 × 10 ^{−13} –1 × 10 ^{−12} [16–18]
Tensile Strength (TS) (MPa)	1–100 [2–4,7,15]	1–100 [16]
Elongation Before Break (EBB) (%)	1–50 [2–4,7], 100 (with plasticizer) [2,7]	1–500 [16]
Young's Modulus (<i>E</i>) (GPa)	0.1–3 [7,15]	1–10

An important criterion for the selection of a crosslinking agent for food applications is that the compound needs to be non-toxic. This eliminates cytotoxic compounds such as glutaraldehyde and epichlorohydrin, which are commonly used to crosslink chitosan [19,20] for industrial membrane applications such as waste water treatment. Similarly, grafting or crosslinking reactions facilitated by 1-ethyl-3-(3-dimethylaminopropyl)carbodiimide with *N*-hydroxysuccinimide [11] are unsuitable since these compounds are not food grade.

Tannic acid has been studied as a crosslinking agent for chitosan films [21], and has shown improvement in WVP and TS. However, tannic acid is a complex, large polyalcohol compared to typical crosslinkers, making it more difficult to understand its effect on film properties. Genipin, an extract from gardenia and jagua fruit, is another option [22,23], and although reported to have herbal benefits and is used for drug delivery [22], it has not yet been approved by the USA Food and Drug Administration. Citric acid is non-toxic and has been used as a crosslinker for chitosan and other polysaccharides for edible films [8,24–26], textiles [27,28], and hydrogels for drug delivery [29–31]. The reactions between chitosan and citric acid take place in the films at temperatures between 110 to 190 °C [8,32], ranging from a few minutes to several hours [8,32,33], with citric acid concentrations of 5 to 30% (of dry polymer weight) [34], and either with [8,35] or without [26,29,32] a catalyst. Recent work on plasticized chitosan films crosslinked with citric acid (1:1 *w/w* chitosan) reports lower water absorption and WVP, but at the expense of lower TS and mechanical modulus [26]. Composite hemicellulose-chitosan foams show improvement in TS [33] after crosslinking with citric acid.

The research on chitosan edible films crosslinked by citric acid has thus far performed the crosslinking in a homogeneous manner [8,26,32]. That is, with a filmogenic solution containing citric

acid in addition to acetic acid. However, this method might not be the most appropriate. A study on the effect of heating chitosan films has shown amidization reactions occur with the acids used in the preparation [36]. However, at 60 °C, citric acid does not appear to react with the amine of chitosan [36] to the extent that acetic acid and propionic acid do. Therefore, in order to avoid competing reactions between acetic and citric acid, acetic acid should be removed prior to the incorporation of the crosslinker into the polymer matrix. Such a multi-step process is referred to as heterogeneous crosslinking, and has been performed with epichlorohydrin [19], glutaraldehyde [19,37,38] and genipin [23] for chitosan.

In this work, the potential crosslinking of chitosan with citric acid using the heterogeneous procedure was investigated. Two crosslinkers were used: citric acid and a model crosslinker, glutaraldehyde (GTA). Additionally, homogeneous and heterogeneous methods were compared. While Fourier transform infrared spectroscopy is an effective technique for studying changes to chemical structure, such as the detection of new amide [33] or ester [24,35] bonds, the method cannot provide distinction between grafting and crosslinking. In this work, crosslinking was examined by studying the viscoelastic properties (storage modulus, E' , loss modulus, E'' , and $\tan\delta$) using dynamic mechanical analysis (DMA) by considering principles of the rubber elasticity theory. This same approach has been used previously for analyzing the crosslinking characteristics of various polysaccharide and protein materials, such as methyl cellulose crosslinked with GTA [39], whey proteins with formaldehyde [40], starch with trisodium trimetaphosphate [41], and chitosan hydrogels crosslinked with genipin [42]. Figure 2 illustrates the postulated covalent crosslinking by conversion of primary amine to amide upon heat treatment of a chitosan film with citric acid, irrespective of film preparation by either the homogeneous or heterogeneous crosslinking methods. Figure 2 also illustrates the ionic crosslinking in a chitosan—citrate film with no heat treatment.

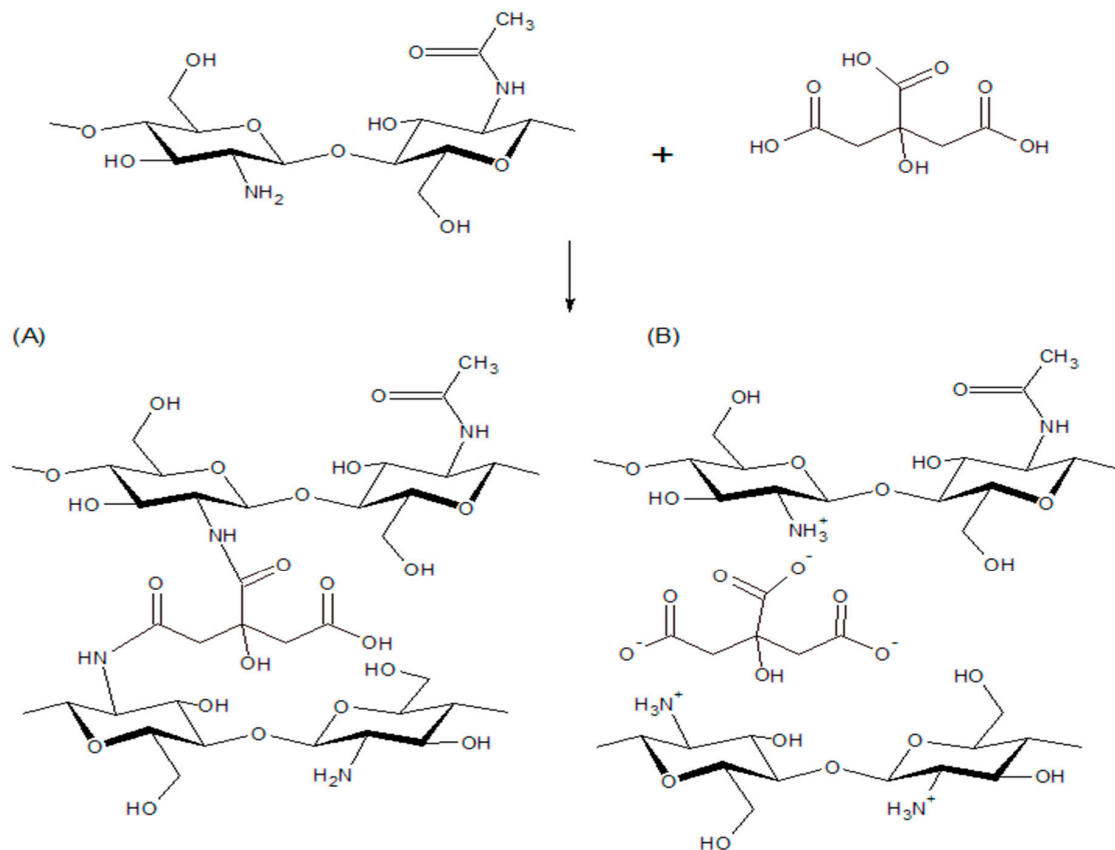


Figure 2. (A) Postulated covalent crosslinking of chitosan and citric acid with heat treatment and (B) electrostatic bonding and ionic crosslinking between the protonated amine and carboxylate ion of a non-heat treated chitosan citrate film.

2. Materials and Methods

2.1. Materials

Chitosan ($M_v = 50\text{--}190$ kDa, 20–300 cP, 1 wt.% in 1% acetic acid solution at 25 °C, 75 to 85% DD), acetic acid (>99.7%), and glutaraldehyde (Grade II, 25 wt.% aqueous solution) were purchased from Sigma Aldrich (St. Louis, MO, USA). Citric acid (>99.5%) was obtained from Fisher Scientific (Fair Lawn, NJ, USA) and sodium hydroxide (>95%) from EMD Chemicals (Gibbstown, NJ, USA). All reagents were used as received without further modification. Ultra-pure water was used in the film preparation process.

2.2. Film Preparation

The following films were prepared: (i) neat films, (ii) neutralized films, (iii) films with different GTA concentration crosslinked homogeneously, (iv) films with different GTA concentration crosslinked heterogeneously, (v) films with citric acid prepared heterogeneously without subsequent heat treatment, and (vi) films with citric acid prepared heterogeneously with subsequent heat treatment. Table 2 lists the film types, their crosslinker content, and their corresponding code names.

Neat chitosan films were made by the solvent casting method with 300 mL of filmogenic solutions of 2% (w/v) chitosan in 2% (v/v) aqueous acetic acid. After mixing, solutions were filtered through cheesecloth to remove undissolved material and impurities and subsequently degassed using a vacuum aspirator to reduce dissolved gases. The solutions were cast on glass trays (16 × 30 cm) at ambient conditions. Temperature and relative humidity (RH) conditions ranged from 18–23 °C and 20–25%, respectively, and were monitored by a thermo-hygrometer (SMART², InterTAN Inc., Barrie, ON, Canada). The films required approximately 48 to 60 h to completely dry and form.

Neutralized films were prepared by submerging dried neat films in solutions of 0.2 M NaOH for 30 min, and were then thoroughly rinsed with ultra-pure water until the pH of the diluent reached that of water. Excess water was wiped off the surface, and the wet neutralized films were firmly clamped between a frame and glass plate to maintain shape and dimensions and avoid shrinkage [43], and were then dried in an environmental chamber at 23 °C and 50% RH for 24 h.

Films crosslinked with GTA were prepared via the homogeneous and heterogeneous methods. For homogeneously crosslinked films, denoted as GTA-HOM from now on, the filmogenic solutions were prepared as the neat films; however, prior to casting, a predetermined amount of GTA (3, 6, 12 wt.% of chitosan) was slowly added to the solution. The crosslinking reactions proceeded instantaneously and continued during the drying phase, which took approximately 24 to 36 h. Heterogeneously crosslinked films, referred to as GTA-HET from now on, were prepared by immersing dried neutralized films in 200 mL GTA aqueous solutions for 24 h at ambient conditions, where the GTA (6, 12 wt.% of dried neutralized film) absorbed into the film and reacted with the chitosan. The longer duration for crosslinking in the heterogeneous method is due to slower reaction kinetics controlled by the lower rate of diffusion of GTA into the already formed film [38]. The wet GTA-HET films were dried for 24 h in the environmental chamber (23 °C and 50% RH). The GTA-containing films changed color to an orange-hue, as expected and reported previously [44].

Films containing citric acid (denoted as CA films) were prepared via the heterogeneous method. Dried neutralized films were immersed 200 mL of citric acid aqueous solutions for 5 h at ambient conditions. The concentration of citric acid was 15% (w/w dried neutralized film). The wet CA film was clamped and dried for 24 h in the environmental chamber. The films were partitioned and one piece was heat treated, (denoted as CA-HT films), at 150 °C for 0.5 h in an attempt to induce covalent crosslinking. These heat treatment conditions were chosen based on the information reported in the literature [8,32] and by taking into consideration that citric acid degrades after melting above 160 °C [29]. Based on the DD of the chitosan provided by the supplier, the approximate ratio of $[\text{NH}_2]$ to $[\text{COOH}]$ could vary from 0.88 to 0.99, near stoichiometric ratio.

Table 2. Chitosan Film Types.

Film	Code Name
Neat	Neat
Neutralized	Neutralized
Homogeneously crosslinked with 3% (<i>w/w</i>) glutaraldehyde (GTA)	GTA-HOM-3
Homogeneously crosslinked with 6% (<i>w/w</i>) glutaraldehyde	GTA-HOM-6
Homogeneously crosslinked with 12% (<i>w/w</i>) glutaraldehyde	GTA-HOM-12
Heterogeneously crosslinked with 6% (<i>w/w</i>) glutaraldehyde	GTA-HET-6
Heterogeneously crosslinked with 12% (<i>w/w</i>) glutaraldehyde	GTA-HET-12
Heterogeneously prepared with 15% (<i>w/w</i>) citric acid (CA)	CA
Heterogeneously prepared with 15% (<i>w/w</i>) citric acid, heat treated	CA-HT

2.3. Dynamic Mechanical Analysis

The viscoelastic properties of the films were measured by temperature-ramp experiments in tensile mode using a TA DMA Q800 (TA Instruments, New Castle, DE, USA) following the guidance of ASTM D5206 (Standard Test Method for Plastics: Dynamic Mechanical Properties: In Tension). The specimen dimensions were 5.5 ± 0.4 mm (width) \times 10.0 ± 0.1 mm (gauge length). A preload force of 1 N was applied during gauge length measurements. The thickness of the films ranged between 80 and 120 μ m, and were measured using a digital micrometer (0.002 mm accuracy, Marathon Watch Company, Richmond Hill, ON, Canada).

Films were heated at a constant rate of 3 $^{\circ}$ C/min, at a fixed frequency of 1 Hz and constant strain of 0.15%. Preliminary strain-ramp tests showed that neat, neutralized, and crosslinked films displayed a linear viscoelastic response above a strain of 0.12% at 30 $^{\circ}$ C. The films were tested in triplicate, with the exception of GTA films which were tested with single or duplicate measurements. The viscoelastic properties measured by the DMA and used for the analysis included storage modulus, E' , loss modulus, E'' , and $\tan\delta = E''/E'$.

The influence of absorbed water in the films on the viscoelastic properties was also evaluated by preheating the specimens prior to DMA. The specimens were heated at 140 $^{\circ}$ C for 10 min without any strain, followed by cooling to room temperature, and then conducting the tests as per the above conditions. DMA tests are referred to film specimen with or without preheating.

Peak fitting was performed on the $\tan\delta$ curves. The $\tan\delta$ peaks were fitted with a constant baseline, whose value was chosen as the minimum $\tan\delta$ value for each specific plot. Fitting was performed with OriginPro 8's Peak Analyzer feature, where the final fit was based on the minimization of chi-square and visual inspection of the fitted and experimental curves. The peak center and full width at half maximum (FWHM) values were statistically evaluated using the Least Significant Difference (LSD) test with a significance level of $\alpha = 0.1$.

3. Results and Discussion

3.1. Description of Viscoelastic Behavior of Neat, Neutralized and CA Films

The plots of non-preheated neat, neutralized, CA and CA-HT films are shown in Figure 3. Their temperature-dependent viscoelastic behaviors are now briefly described. (Note: The ranges of temperatures discussed are based on trends collectively observed from replicate runs.) The E' of neat films decreased relatively linearly from 30 $^{\circ}$ C to approximately 100 $^{\circ}$ C, and then either plateaued or reached a local minimum, increased to approximately 120–140 $^{\circ}$ C, decreased to a local minimum near 160–180 $^{\circ}$ C and increased upon further heating. The corresponding E'' increased from 30 $^{\circ}$ C and passed through a shoulder peak until it reached a local maximum near 100 $^{\circ}$ C, decreased to a local minimum near 130–140 $^{\circ}$ C, and then increased to a maximum at 150–160 $^{\circ}$ C. The corresponding $\tan\delta$ increased from 30 $^{\circ}$ C to a small, broad peak near 100 $^{\circ}$ C along with a smaller secondary peak, reached a minimum between 120–130 $^{\circ}$ C and increased to a maximum near 160–170 $^{\circ}$ C.

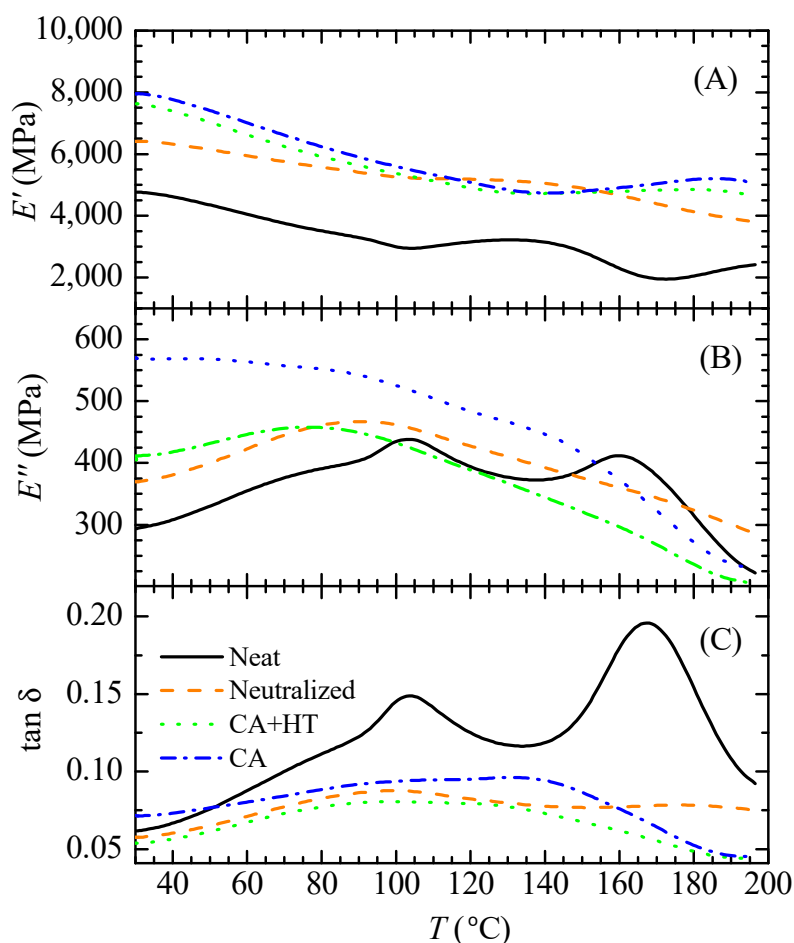


Figure 3. The plots of (A) storage modulus, (B) loss modulus, and (C) $\tan\delta$ against temperature of neat, neutralized, CA, and CA-HT films with no preheating.

The $\tan\delta$ peak near 100 °C is the water induced relaxation peak arising from desorption and subsequent evaporation of water molecules [45]. The additional secondary-peak, centered around 110 °C, was likely induced by the presence of acetic acid, as it was absent from the scans of neutralized, GTA (Section 3.3) and CA films. It may be related to the σ -type conduction of acetate ions and protons observed in isochronal dielectric measurements [46] in the temperature range of -10 to 150 °C of neutralized and non-neutralized chitosan films.

The E' for neutralized films decreased linearly from 30 °C to approximately 100 °C, then plateaued until approximately 160 °C, and thereafter decreased. The corresponding $\tan\delta$ increased from 30 °C to a broad maximum near 100 °C, decreased to a local minimum near 140–160 °C before it increased to a weak maximum near 180 °C. For CA and CA-HT films, a sufficient amount of similarity in their DMA scans warrant a joint description and discussion. The E' of the CA and CA-HT films decreased from 30 °C to a minimum near 140 °C, and then increased to a local maximum between 170–190 °C. For E'' , a local maximum appeared near 80 °C, passed through a shoulder peak near 140 °C and declined thereafter. The corresponding $\tan\delta$ plots showed an increase up to 100–120 °C at which point the curve either plateaued or displayed a second local maximum between 120–140 °C.

The E' values at 35 °C and 195 °C extracted from the plots of non-preheated neat, neutralized, CA, and CA-HT films are listed in Table 3. The two temperature levels are near ambient conditions, and onset of degradation, respectively. The $\tan\delta$ peak values and corresponding temperatures are also listed in Table 3 (last four columns). The low temperature peak near 100 °C is designated as ‘peak 1’ and the high temperature peak near 160 °C is designated as ‘peak 2’.

Comparison of the E' values provides an assessment of material stiffness, which is related to crosslinking as per the rubber elasticity theory. Increasing crosslink density, or decreasing the average molecular weight between crosslinks, increases E' in the rubbery-region of a material [47,48]. The $\tan\delta$ glass-transition relaxation peak broadens as the distribution of relaxation times increases and, it shifts to higher temperatures as crosslinking increases the glass transition temperature, T_g . The drop in E' with temperature across the glass-rubber transition for polysaccharides does not occur over several magnitudes as it does with thermoplastics or rubbers. The applicability of rubber elasticity theory on polysaccharide gels has been questioned as high stiffness of a material creates an internal energy dependence to the overall change in free energy when it is mechanically deformed, in violation of the entropic assumption of the theory [49]. Therefore, a quantitative estimate of crosslink density is avoided here, and only evaluation of E' and $\tan\delta$ is used.

From Table 3 it can be seen that: (i) neat films had a lower E' overall, (ii) E' and $\tan\delta$ of CA and CA-HT films were not statistically different from one another, and (iii) the E' (195 °C) values of CA and CA-HT films were not statistically different compared to neutralized films. Regarding (i), the results were as expected: neutralized films are stiffer than neat films because of a lower absorbed water content of approximately 3% [50], which results in an increase in stronger inter- and intramolecular hydrogen bonds. Crosslinking by GTA restricts chain mobility, hence the higher E' of GTA-HOM films compared to neat films. For (ii), these results demonstrate that heat treatment followed by 72 h of conditioning did not influence the viscoelastic behavior of films with citric acid. Regarding (iii), this observation shows that citric acid did not influence the properties relative to neutralized films during the approach towards the glass transition as anticipated. An example of such an observation was made with a DMA frequency sweep of a heterogeneously crosslinked chitosan-genipin film studied under physiological conditions that exhibited a storage modulus value more than double that of its neutralized counterpart [42]. Any differences between neutralized and CA films could be structure related, and not necessarily related to crosslinking. For instance, X-ray diffraction (XRD) scans of chitosan films cast with citric acid displayed a more amorphous structure than chitosan acetate films [36]. Since polymers with a higher crystallinity typically display greater storage modulus [47], it might be possible that an increase in amorphous structure caused by citric acid had a counterbalancing effect on the increase in rigidity from crosslinking, and thus the difference in E' (195 °C) of neutralized and CA films was not statistically significant. Neutralization does decrease the degree of crystallinity [50], by about 6% [51] compared to neat films.

Comparing the crosslinked and non-crosslinked forms of a material does have some challenges. If the degree of physical entanglements is high it could mask the detection of new covalent crosslinks in the rubbery-plateau region if the degree of covalent junctures is low. Changes to the storage modulus in this region from crosslinking become more observable when tested using lower frequencies [52], and 1 Hz is sufficiently low. While crosslinking is expected to increase E' in the rubbery region, it does not always increase it in the glassy region, as demonstrated by photo-crosslinked polyacrylate membranes [48]. For this reason, E' (35 °C) is considered less of an indicator for crosslinking here, especially as E' (35 °C) of CA and CA-HT are not significantly different.

The crosslinking procedure can influence the degree of crystallinity and the type of bond between the crosslinker and chitosan [19,37]. For example, heterogeneous crosslinking with chitosan-glutaraldehyde does not reduce crystallinity to the extent that the homogeneous procedure does [19], and it is hypothesized that heterogeneous crosslinking mostly occurs at the surface [19] and in the amorphous regions of the polymer matrix [37]. It is similarly expected that citric acid will absorb and react mostly at the surface and amorphous domains of the films.

Preload forces may have some impact on measured viscoelastic properties, especially on softer, biological materials [53]. Strain hardening from preloading can be avoided with strain-rate measurements which negate the use of a trigger force before the measurements. Bartolini et al. [54] studied the viscoelastic response of nano-indented poly(dimethylsiloxane) strips and found that the apparent elastic moduli of previously strained samples were lower than non pre-strained samples.

Here, the 1 N force applied to the specimens during gauge length measurements is unlikely to make a great impact, as it is less than the net force applied to the specimens for 0.15% strain. It is possible that the static force applied during dynamic moduli measurements could affect the different film types to different degrees, thereby creating a bias in the data.

Chitosan films are non-isotropic with a significant degree of variation of density, crystallinity, and chemical structure throughout. This will impact the apparent mechanical moduli values which are determined as a bulk quantity, averaged over the specimen volume. Inhomogeneities within the crosslinked films can be probed using microscale techniques such as nano-indentation, where the indenting load is applied cyclically, either at a constant or increasing load rate [55,56]. This could be considered for assessing differences in heterogeneity between neat, neutralized and CA films.

Table 3. Characteristics of the dynamic mechanical analysis (DMA) curves for film specimens with no-preheating (see Table 2 for film code names).

Film	Parameter	E'	E'	tan δ Peak 1		tan δ Peak 2	
		(35 °C)	(195 °C)	T	tan δ	T	tan δ
		(MPa)	(MPa)	(°C)		(°C)	
Neat	mean	5071 ^a	2382 ^a	102.0 ^a	0.129 ^a	164.8 ^a	0.216 ^a
	±	432	127	2.8	0.015	2.8	0.045
	COV* (%)	8.5	5.3	2.7	11.7	1.7	21.1
	n	6	6	6	6	6	6
Neutralized	mean	6665 ^b	4143 ^b	106.7 ^a	0.089 ^b	187.6 ^b	0.078 ^b
	±	728	334	12.9	0.003	9.8	0.001
	COV* (%)	11	8	12.1	3.4	5.2	1.7
	n	5	5	5	5	4	5
CA	mean	7588 ^c	4727 ^c	106.9 ^a	0.099 ^b	130.2 ^c	0.097 ^{b,c}
	±	489	349	8.9	0.016	8.4	0.026
	COV* (%)	6.4	7.4	8.3	16.4	6.5	26.3
	n	3	3	3	3	2	2
CA+HT	mean	7605 ^c	4479 ^{b,c}	104.2 ^a	0.088 ^b	131.1 ^c	0.096 ^c
	±	871	635	4.6	0.005	-	-
	COV* (%)	11.5	14.2	4.4	5.5	-	-
	n	4	4	4	4	1	1
GTA-HOM-3	$n = 1$	5123	2475	106.5	0.156	165.7	0.201
GTA-HOM-6	$n = 1$	6222	3367	96.1	0.110	168.9	0.110
GTA-HOM-12	$n = 1$	5882	3160	97.3	0.090	167.0	0.091

* COV—Coefficient of Variation. Significant statistical difference between means is indicated by different superscripted letters (LSD test, $\alpha = 0.1$).

3.2. Effect of Preheating Film Specimens and Thermal Treatment on CA Films

The effects of heat treatment on CA films and preheating on films are now discussed. Scans of preheated neat, neutralized, CA, and CA-HT films are shown in Figure 4. At low temperatures, E' increased relative to non-preheated films by approximately 2000 MPa and the slope of $\Delta E' / \Delta T$ was greater for the majority of the scan. Above 170 °C the storage modulus plots of the non-preheated and preheated scans merged and overlapped (or see Park and Ruckenstein [39] for similar observation with methylcellulose). This is due to the difference in water content becoming less with increasing temperature. Additionally, preheating reduced peak 1 from values in the range of 0.89–0.99 down to 0.52–0.59 for neutralized and CA films, respectively. For the full set of tan δ and E' values of preheated neat, neutralized, CA and CA-HT films, see Table 4.

Table 4. Characteristics of DMA curves for Preheated Specimens (see Table 2 for film code names).

Film	Parameter	E'	E'	$\tan\delta$ Peak 1		$\tan\delta$ Peak 2	
		(35 °C)	(195 °C)	T	$\tan\delta$	T	$\tan\delta$
		(MPa)	(MPa)	(°C)		(°C)	
Neat	mean	7826 ^a	2289 ^a	-	-	169.3 ^a	0.213 ^a
	s	427	152	-	-	4.2	0.034
	COV* (%)	5.5	6.6	-	-	2.5	16.0
	n	4	4	0	0	4	4
Neutralized	mean	9384 ^b	4162 ^b	124.1 ^a	0.059 ^a	187.2 ^b	0.078 ^b
	s	859	385	3.8	0.002	5.5	0.003
	COV (%)	6.7	6.8	2.5	3.4	2.3	2.6
	n	6	6	6	6	6	6
CA	mean	9982 ^b	4348 ^b	117.8 ^b	0.059 ^{a,b}	166.5 ^a	0.061 ^c
	s	220	93	1.0	0.005	1.1	0.005
	COV (%)	2.2	2.1	0.8	8.3	0.7	9.0
	n	2	2	2	2	2	2
CA+HT	mean	9351 ^b	4612 ^b	125.8 ^{a,b}	0.050 ^b	165.3 ^a	0.051 ^c
	s	609	244	10	0.004	3.2	0.004
	COV (%)	6.5	5.2	7.9	8.0	1.9	8.8
	n	3	3	3	3	3	3
GTA-HOM-3	mean	9119	2749	97.3	0.060	175.3	0.167
	s	282.1	159.3	5.8	0.000	0.5	0.008
	n	2	2	2	2	2	2
GTA-HOM-6	$n = 1$	9740	3162	92.4	0.068	181.6	0.101
GTA-HOM-12	$n = 1$	9413	3584	77.9	0.067	191.8	0.080

* COV—Coefficient of Variation. Significant statistical difference between means is indicated by different superscripted letters (LSD test, $\alpha = 0.1$).

Since the film specimens were heated by ramping in the DMA, and CA-HT films were thermally treated prior to DMA testing, it is important to consider changes to chemistry and chain structure following heat treatment and their subsequent effects on mechanical properties. Infrared spectroscopy studies reveal an increase in the intensity of bands corresponding to secondary amine ($-\text{NH}-$) (amide II) [21] and amide-carbonyl ($-\text{N}-\text{C}=\text{O}$) (amide I) [21,36] at approximately 1560 and 1650 cm^{-1} , respectively, as a consequence of heating. They also show a simultaneous decrease in protonated amine and carboxylate ion peaks at approximately 1515/1615 and 1555 cm^{-1} , respectively. As stated earlier, the potential reactions between chitosan amine and carboxyl groups from residual acetic acid is the main motive for neutralizing the films prior to the absorption of citric acid into the matrix: to avoid competition of amidization between the two acids. Further evidence of reaction resulting from conditioning at high temperatures (>100 °C) is reduced film solubility in water [21] and acid aqueous solutions [21,57], which agrees with the effect of amidization as protonation of the amine is necessary for chitosan dissolution.

Some authors report an overall decrease in crystallinity [36] with heating. In this situation, the higher ratio of amorphous to crystalline regions would likely strengthen the appearance of T_g and cause it to shift to higher temperatures and decrease E' . If there is such a reduction in crystallinity in preheated or heat treated films here, it is negligible with respect to the error associated with experimentation as the E' (195 °C) of preheated and non-preheated scans are not significantly different. Other studies report a transformation from the 'tendon' (hydrated) to the 'annealed' (anhydrous) crystal structure [57] after heating. Despite all potential changes to physico-chemical and structural properties from preheating or heat treatment that may affect mechanical properties, they are less likely to be detectable in the glassy state by the more pronounced effect of increased rigidity when absorbed

water is evaporated out. In short, no effects from changes to crystal structure or crystallinity from heating were observed here.

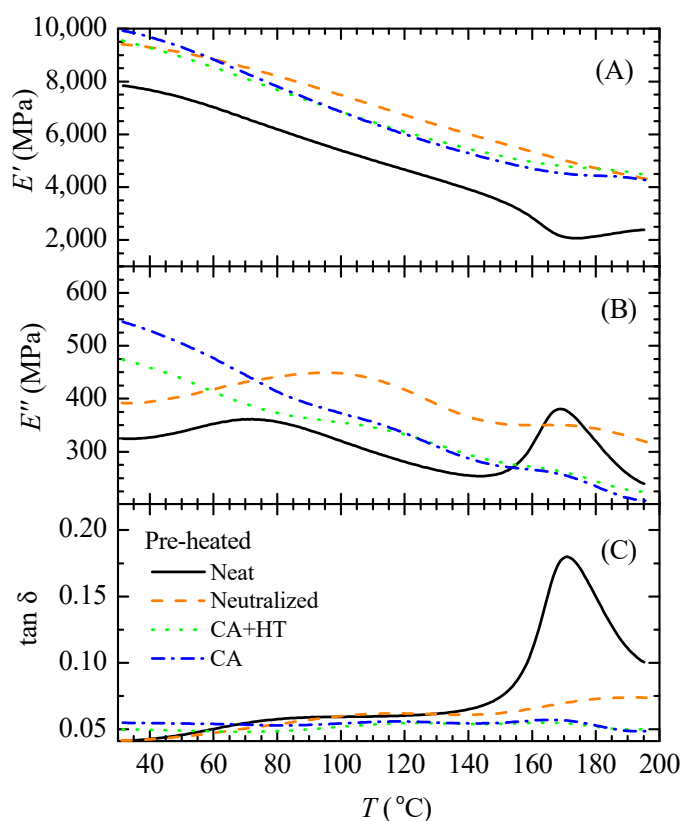


Figure 4. The plots of (A) storage modulus, (B) loss modulus, and (C) $\tan\delta$ against temperature of preheated neat, neutralized, CA, and CA-HT films.

3.3. GTA-Crosslinked Films

The $\tan\delta$ and E' values from the non-preheated and preheated scans of GTA-HOM films are listed in Tables 3 and 4, respectively; see Table 2 for the film names. The plots for preheated scans for GTA-HOM films are shown in Figure 5, and plots of non-preheated scans are shown in Figure A1 in the Appendix A. Comparisons with neat films, and the effect of GTA concentration are now discussed. The film with the lowest concentration, GTA-HOM-3, displayed similar quantitative and qualitative viscoelastic behavior to the neat films. For both non-preheated and preheated conditions, the E' (195 °C) values of GTA-HOM films exceed those of neat films, as expected with crosslinked films. Increasing the concentration from 3 to 12% caused the following changes: (i) a decrease in magnitude of peak 1 (non-preheated scans) as amide/imide formation would reduce H-bonding capacity, (ii) a decrease in $\tan\delta$ peak 2 magnitude and a shift to higher temperatures (Table 4), and (iii) an overall increase in E' . The E' , E'' and $\tan\delta$ curves for preheated GTA-HOM-6 and -12 films overlapped reasonably well, indicating marginal differences in the degree of crosslinking above 6% GTA. A systematic increase in E' (195 °C) with an increase in GTA concentration was observed for preheated GTA-HOM films. However, this was not seen in the non-preheated GTA-HOM specimens, which may be related to the stiffness of the polymer chain. Park et al. [39] did not observe significant changes to the glass transition peak in their DMA $\tan\delta$ scans of methylcellulose-GTA crosslinked hydrogels, and they claimed that the high rigidity of the polysaccharide backbone prevents any indication of changes induced by covalent crosslinking.

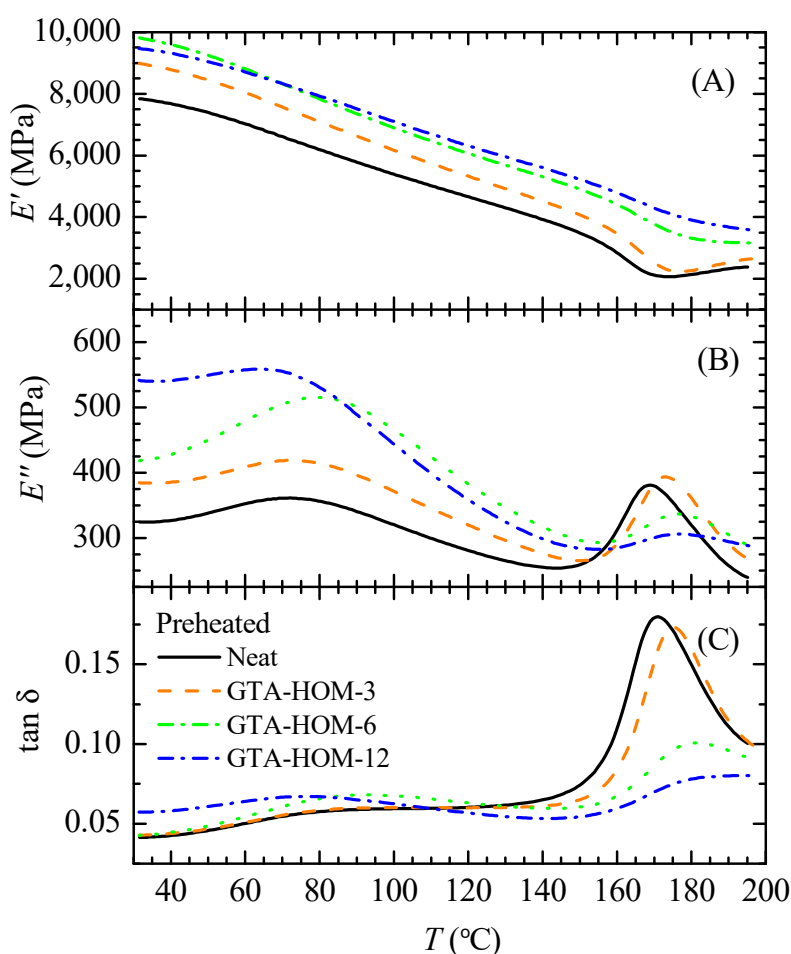


Figure 5. The plots of (A) storage modulus, (B) loss modulus, and (C) $\tan\delta$ against temperature of preheated 3, 6, and 12% GTA-HOM films and a neat chitosan film.

In addition to GTA-HOM films, heterogeneously prepared GTA films were also investigated. (DMA studies of heterogeneously crosslinked chitosan-glutaraldehyde films are seldom reported but are still available in the literature [58].) Figure 6 shows the DMA scans of GTA-HET-6 and GTA-HET-12 films. For these films, the maximum temperature of the scan was increased from 200 to 220 °C to test the temperature-DMA limits of the chitosan films. Despite being more brittle, the E' values of the GTA-HET crosslinked films were less than both the homogeneously prepared GTA and neutralized films within the majority of the temperature range recorded, as shown in Figure 6. This would suggest that producing films heterogeneously might have cleaved the polymer chains while simultaneously crosslinking them, mostly at the exterior [19]. New bonds formed with glutaraldehyde may either be imines, or a combination of imine and Michael-type adducts, for heterogeneous versus homogeneous crosslinking, respectively [19]. The difference in bond formation and majority of crosslinking at the exterior of the film might account for the extra brittleness exhibited by GTA-HET films.

The $\tan\delta$ peak 2 was not visible for the GTA-HET films, but rather a new, broad peak with an onset near 170 °C began to emerge, whose center was out of the measured temperature range. This peak could be more representative of a glass-rubber transition which is speculated to exist within the film degradation range. The degradation of neutralized chitosan films typically begins near 200 °C and reaches a maximum degradation rate near 275 °C [43]. For our neutralized films, only a 1% mass loss was found between 200 and 250 °C and the differential thermogravimetric analysis peak was at 290 °C. It cannot be ruled out that the GTA-HET peak onset at 170 °C could be due to an earlier onset of degradation, as crosslinking with GTA [58] has been found to do. However, in the case of heterogeneously crosslinked chitosan membranes formed by electrospinning, thermogravimetric

analysis scans by Correia et al. [59] did not demonstrate differences between neutralized chitosan films and ethanol neutralized-heterogeneously crosslinked GTA membranes, showing that heterogeneous crosslinking with GTA does not necessarily lower the decomposition onset temperature.

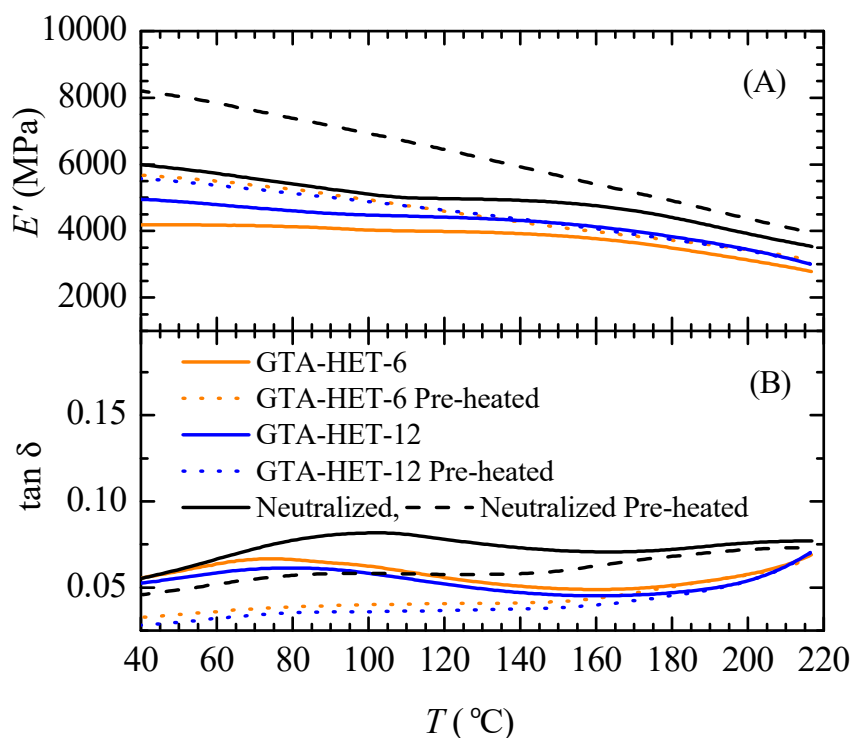


Figure 6. The plots of (A) storage modulus and (B) $\tan\delta$ against temperature of non-preheated and preheated scans of 6 and 12% GTA-HET films.

3.4. Analysis of $\tan\delta$ and Relation to Crosslinking

To evaluate the relaxation properties of the films further, peak deconvolution was performed on the $\tan\delta$ curves to obtain a more accurate peak center and to estimate the FWHM (units of temperature). If $\tan\delta$ peak 2 is related to the glass transition, one would expect peak widening as a consequence of crosslinking and a shift to higher temperatures.

The $\tan\delta$ peak 2 deconvolution analysis is presented in Table 5. The peak 2 FWHM values of the neutralized films were higher (statistically significant) than those of the CA films for both preheated and non-preheated specimens, contrary to expectations of peak broadening with the addition of citric acid and formation of covalent crosslinks. Furthermore, the FWHM values of preheated CA and CA-HT films were not significantly different, which suggests that thermal treatment likely did not change the bonding type from ionic to covalent, just as the lack of difference in E' values previously indicated, as discussed in Section 3.1. By contrast, the peak width of GTA-HOM films increased from 35 to 59 °C by increasing GTA concentration from 3 to 12%, and peak 2 moved to higher temperatures, according to expectations of an increase in crosslink density.

The height of the $\tan\delta$ peak 2 diminished from 0.213 ± 0.045 for neat to 0.078 ± 0.01 for neutralized films. The reason for this drop may be due to changes to the chemical nature of the films. Gartner et al. [50] speculated that the origins of this relaxation peak are from electrostatic, ionic interactions between the conjugate base of the solvating acid and the protonated amine. They compared the $\tan\delta$ properties of neat and neutralized films made from acetic and hydrochloric acid using DMA, and similar $\tan\delta$ temperature-dependence of their chitosan acetate film was found with this study. Their ^{15}N nuclear magnetic resonance (NMR) scans [50] provide supporting evidence for the electrostatic interactions by showing shifts in the peak correlated with the amine group of the HCl-prepared neutralized film to a position approximately that observed for the unprotonated chitosan

powder, thus suggesting the conversion from $-\text{NH}_3^+$ back to $-\text{NH}_2$ [50] following treatment with NaOH. Thus, the lower height of $\tan\delta$ peak 2 for neutralized chitosan films observed in this study makes the hypothesis of ionic effects responsible for the relaxation peak as more plausible (and less likely to be the T_g).

Preheating film specimens prior to DMA scans did not significantly change the $\tan\delta$ peak 2 height or position for neat and neutralized films, as shown in Table 5. By contrast, Sakurai et al. [60] found that preheating their chitosan films at 180 °C caused the $\tan\delta$ peak at 150 °C to subside compared to non-preheated film, and instead a new peak emerged at 205 °C, which they speculated was closer to the true T_g , and thus argued the peak at 150 °C was from a pseudo-stable state of the polymer chains. The removal of plasticization effects from water would increase T_g ; however, as this was not observed here for T (peak 2) of neat and neutralized films, this casts further doubt on the plausibility that the origin of peak 2 being the glass-rubber transition. Moreover, with preheating of neutralized specimens, peak 2 became more observable, indicating a partial masking effect caused by absorbed water and the water-induced relaxation peak.

To further elucidate the nature of the $\tan\delta$ peak 2, films containing 15% citric acid were prepared homogeneously, with a 2% acetic acid solution. This film was not subsequently heat treated so the crosslinking was ionic. The similarity of the $\tan\delta$ curves of the homogeneously and heterogeneously prepared CA films sufficiently demonstrated that the shift of the peak 2 center from 165 to 130 °C with the incorporation of citric acid into the films was independent of the film preparation method. See Figure A2 in the Appendix A. This further supports the notion that the high temperature peak is from ionic effects, as citric acid will be in its conjugate form in a film crosslinked homogeneously. The difference between the viscoelastic properties of a chitosan acetate film and a chitosan citrate film is that preheating has a more significant effect on T (peak 2) for the latter than the former.

Table 5. Peak Deconvolution, Fitting Data for $\tan\delta$ Peak 2 (see also Tables 2–4).

Film Type	Preheat	Parameter	Baseline	Center (°C)	FWHM	Height
Neat	N	mean	0.068 ^a	166.0 ^a	36.5 ^a	0.130 ^a
		±	0.005	2.9	2.6	0.034
Neat	Y	mean	0.052 ^b	177.2 ^b	29.9 ^a	0.116 ^a
		±	0.008	6.5	4.4	0.047
Neutralized	N	mean	0.057 ^b	188.8 ^c	105.5 ^b	0.021 ^{b,c}
		±	0.002	12.2	29.1	0.002
Neutralized	Y	mean	0.029 ^c	188.5 ^c	67.9 ^c	0.048 ^c
		±	0.006	3.4	4.8	0.008
CA+HT	N	mean	0.046 ^b	137.6 ^d	56.8 ^c	0.013 ^b
		±	0.002	5.7	3.4	0.002
CA+HT	Y	mean	0.045 ^b	168.3 ^a	32.2 ^a	0.006 ^b
		±	0.006	4.1	7.6	0.004
CA	N	mean	0.046 ^b	146.2 ^d	44.7 ^a	0.024 ^b
		±	0.004	2.0	5.5	0.004
CA	Y	mean	0.045 ^b	173.3 ^{a,b}	44.1 ^a	0.012 ^b
		±	0.005	13.3	27.8	0.008

Significant statistical difference between means is indicated by different superscripted letters (LSD test, $\alpha = 0.1$). FWHM: full width at half maximum.

4. Conclusions

The viscoelastic properties, namely the E' , E'' , and $\tan\delta$ of chitosan films were investigated to gain insights on the presence of potential covalent crosslinking between citric acid and chitosan. According to the rubbery elasticity theory for crosslinked polymers, the storage modulus is expected to be higher as the polymer approaches and enters into the rubbery region, due to a lower molecular

weight between crosslinks. While the effect of crosslinking for the model GTA films was demonstrated with respect to E' , no statistical difference was observed for E' between CA, CA-HT, and neutralized chitosan films near 200 °C suggesting that the post thermal treatment of CA films did not induce covalent crosslinking and the interaction between the chitosan amine and CA remained ionic. Furthermore, the difference in E' at temperatures above 170 °C for the preheated and non-preheated film specimens was negligible indicating that moisture did not affect the structure of the chitosan films entering the rubbery region. The $\tan\delta$ peak at high temperature (peak 2) was also used as an indicator for crosslinking and the glass transition. The $\tan\delta$ peak 2 of GTA-HOM films shifted to higher temperatures which seemed supportive of an increase in glass transition temperature. However, other changes to $\tan\delta$ from neutralization and the addition of citric acid indicate that the $\tan\delta$ peak 2 is more likely related to ionic bonding. Peak fitting analysis of $\tan\delta$ peak 2 showed that neither the presence of citric acid nor thermal treatment of CA films resulted in the broadening of the peak as would have been expected for an increase in distribution of relaxation times with crosslinking. This was also confirmed by a quantitative and qualitative similarity of the $\tan\delta$ plots of homogeneously and heterogeneously prepared chitosan-citrate and CA films. The high temperature $\tan\delta$ relaxation peak shifted from 170 °C for the neat film down to 130 °C for the CA films, irrespective of the CA film preparation method (homogeneous or heterogeneous). Thus, the DMA measurements seemed to confirm that the high temperature relaxation peak near 170 °C is phenomenologically connected with the ionic state of the polymer, and not an indication of the glass transition. However GTA-HET films did show the emergence of a weakly defined peak above 200 °C, which is more likely to be correlated with the glass transition than any of the other films. Most notable is that these DMA tests confirmed that the heterogeneous method of producing chitosan films with citric acid has potential, just as it is with other crosslinkers such as GTA, epichlorohydrin, and genipin. This allows for future considerations on how to properly induce covalent crosslinking with citric acid using the heterogeneous procedure. This could be achieved by optimizing heat treatment conditions or utilizing a phosphate-based catalyst.

Author Contributions: J.K. conceived, designed, and performed the experiments with input from C.M. and A.P., who supervised the research. The paper was written by J.K. with contributions from C.M. and A.P.

Funding: Financial support from the Natural Sciences and Engineering Research Council (NSERC) of Canada is gratefully acknowledged.

Conflicts of Interest: The authors declare no conflicts of interest.

Appendix A

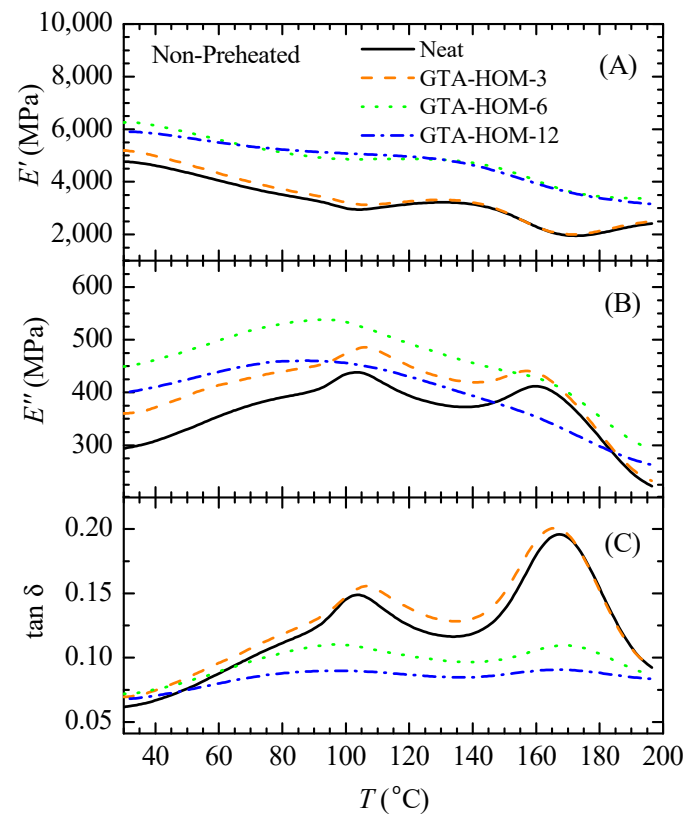


Figure A1. The plots of (A) storage modulus, (B) loss modulus, and (C) $\tan\delta$ against temperature of non-preheated 3, 6, and 12% GTA-HOM films and a neat chitosan film.

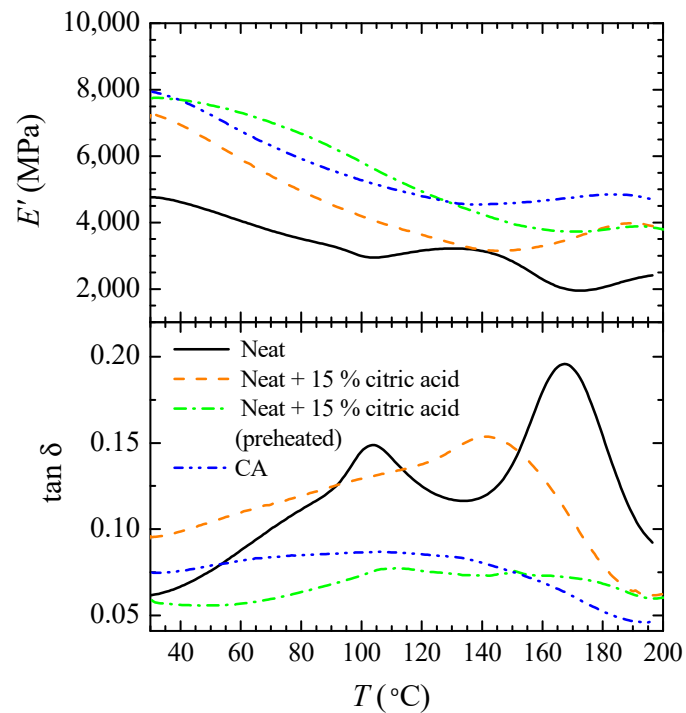


Figure A2. The plots of (A) storage modulus and (B) $\tan\delta$ against temperature of non-preheated specimens of neat film, a neat film with 15% citric acid, a CA film, and a preheated neat film with 15% citric acid.

References

1. Wang, H.; Qian, J.; Ding, F. Emerging Chitosan-Based Films for Food Packaging Applications. *J. Agric. Food Chem.* **2018**, *66*, 395–413. [[CrossRef](#)] [[PubMed](#)]
2. Rhim, J.; Weller, C.; Ham, K. Characteristics of Chitosan Films as Affected by the Type of Solvent Acid. *Food Sci. Food Biotechnol.* **1998**, *7*, 263–268.
3. Park, S.; Marsh, K.; Rhim, J. Characteristics of Different Molecular Weight Chitosan Films Affected by the Type of Organic Solvents. *J. Food Sci.* **2002**, *67*, 194–197. [[CrossRef](#)]
4. Blair, H.; Guthrie, J.; Law, T.; Turkington, P. Chitosan and Modified Chitosan Membranes: I. Preparation and Characterisation. *J. Appl. Polym. Sci.* **1987**, *33*, 641–656. [[CrossRef](#)]
5. Chen, R.; Lin, J.; Yang, M. Relationships Between the Chain Flexibilities of Chitosan Molecules and the Physical Properties of Their Casted Films. *Carbohydr. Polym.* **1994**, *24*, 41–46. [[CrossRef](#)]
6. Wong, D.; Gastineau, F.; Gregorski, K.; Tillin, S.; Pavlath, A. Chitosan-Lipid Films: Microstructure and Surface Energy. *J. Agric. Food Chem.* **1992**, *40*, 540–544. [[CrossRef](#)]
7. Srinivasa, P.; Ramesh, M.; Tharanathan, R. Effect of Plasticizers and Fatty Acids on Mechanical and Permeability Characteristics of Chitosan Films. *Food Hydrocoll.* **2007**, *21*, 1113–1122. [[CrossRef](#)]
8. Möller, H.; Grelier, S.; Pardon, P.; Coma, V. Antimicrobial and Physicochemical Properties of Chitosan-HPMC-Based Films. *J. Agric. Food Chem.* **2004**, *52*, 6585–6591. [[CrossRef](#)] [[PubMed](#)]
9. Bordenave, N.; Grelier, S.; Coma, V. Hydrophobization and Antimicrobial Activity of Chitosan and Paper-Based Packaging Material. *Biomacromolecules* **2010**, *11*, 88–96. [[CrossRef](#)]
10. Höhne, S.; Frenzel, R.; Heppe, A.; Simon, F. Hydrophobic Chitosan Microparticles: Heterogeneous Phase Reaction with Hydrophobic Carbonyl Reagents. *Biomacromolecules* **2007**, *8*, 2051–2058. [[CrossRef](#)]
11. Schreiber, S.; Bozell, J.; Hayes, D.; Zivanovic, S. Introduction of Primary Antioxidant Activity to Chitosan for Application as a Multifunctional Food Packaging Material. *Food Hydrocoll.* **2013**, *33*, 207–214. [[CrossRef](#)]
12. Wu, C.; Tian, J.; Li, S.; Wu, T.; Hu, Y.; Chen, S.; Sugawara, T.; Ye, X. Structural Properties of Films and Rheology of Film-Forming Solutions of Chitosan Gallate for Food Packaging. *Carbohydr. Polym.* **2016**, *146*, 10–19. [[CrossRef](#)]
13. Yoshida, C.; Oliveira, E.; Franco, T. Chitosan Tailor-Made Films: The Effects of Additives on Barrier and Mechanical Properties. *Packag. Technol. Sci.* **2009**, *22*, 161–170. [[CrossRef](#)]
14. Bof, M.; Bordagaray, V.; Locaso, D.; García, M. Chitosan Molecular Weight Effect on Starch-Composite Film Properties. *Food Hydrocoll.* **2015**, *51*, 281–294. [[CrossRef](#)]
15. Rubentheren, V.; Ward, T.; Chee, C.; Nair, P.; Salami, E.; Fearday, C. Effects of Heat Treatment on Chitosan Nanocomposite Film Reinforced with Nanocrystalline Cellulose and Tannic Acid. *Carbohydr. Polym.* **2016**, *140*, 202–208. [[CrossRef](#)]
16. Jimenez, A.; Fabra, M.J.; Talens, P.; Chiralt, A. Edible and Biodegradable Starch Films: A Review. *Food Bioprocess Technol.* **2012**, *5*, 2058–2076. [[CrossRef](#)]
17. Guilbert, S.; Gontard, N.; Gorris, L.G.M. Prolongation of the Shelf-Life of Perishable Food Products using Biodegradable Films and Coatings. *LWT Food Sci. Technol.* **1996**, *29*, 10–17. [[CrossRef](#)]
18. Miller, K.S.; Krochta, J.M. Oxygen and Aroma Barrier Properties of Edible Films: A Review. *Trends Food Sci. Technol.* **1997**, *8*, 228–237. [[CrossRef](#)]
19. Wan, Y.; Creber, K.; Peppley, B.; Bui, V. Ionic Conductivity and Related Properties of Crosslinked Chitosan Membranes. *J. Appl. Polym. Sci.* **2003**, *89*, 306–317. [[CrossRef](#)]
20. Pratt, D.; Wilson, L.; Kozinski, J. Preparation and Sorption Studies of Glutaraldehyde Cross-Linked Chitosan Copolymers. *J. Colloid Interface Sci.* **2013**, *395*, 205–211. [[CrossRef](#)]
21. Rivero, S.; García, M.; Pinotti, A. Heat Treatment to Modify the Structural and Physical Properties of Chitosan-Based Films. *J. Agric. Food Chem.* **2012**, *60*, 492–499. [[CrossRef](#)] [[PubMed](#)]
22. Muzzarelli, R. Genipin-Crosslinked Chitosan Hydrogels as Biomedical and Pharmaceutical Aids. *Carbohydr. Polym.* **2009**, *77*, 1–9. [[CrossRef](#)]
23. Pandis, C.; Madeira, S.; Matos, J.; Kyritsis, A.; Mano, J.; Ribelles, J. Chitosan-Silica Hybrid Porous Membranes. *Mater. Sci. Eng. C* **2014**, *42*, 553–561. [[CrossRef](#)] [[PubMed](#)]
24. Coma, V.; Sebti, I.; Pardon, F.; Pichavant, F.; Deschamps, A. Film Properties from Crosslinking of Cellulosic Derivatives with a Polyfunctional Carboxylic Acid. *Carbohydr. Polym.* **2003**, *51*, 265–271. [[CrossRef](#)]

25. Ghanbarzadeh, B.; Almasi, H.; Entezami, A. Improving the Barrier and Mechanical Properties of Corn Starch-Based Edible Films: Effect of Citric Acid and Carboxymethyl Cellulose. *Ind. Crops Prod.* **2011**, *33*, 229–235. [[CrossRef](#)]
26. Priyadarshi, R.; Sauraj; Kumar, B.; Negi, Y. Chitosan Film Incorporated with Citric Acid and Glycerol as an Active Packaging Material for Extension of Green Chilli Shelf Life. *Carbohydr. Polym.* **2018**, *195*, 329–338. [[CrossRef](#)]
27. Welch, C.; Andrews, B. Ester Crosslinks: A Route to High Performance Nonformaldehyde Finishing of Cotton. *Text. Chem. Color.* **1989**, *21*, 13–17.
28. Gawish, S.; Abo El-Ola, S.; Ramadan, A.; Abou El-Kheir, A. Citric Acid Used as a Crosslinking Agent for the Grafting of Chitosan onto Woolen Fabric. *J. Appl. Polym. Sci.* **2012**, *123*, 3345–3353. [[CrossRef](#)]
29. Demitri, C.; Del Sole, R.; Scalera, F.; Sannino, A.; Vasapollo, G.; Maffezzoli, A.; Ambrosio, L.; Nicolais, L. Novel Superabsorbent Cellulose-Based Hydrogels Crosslinked with Citric Acid. *J. Appl. Polym. Sci.* **2008**, *110*, 2453–2460. [[CrossRef](#)]
30. Fahmy, H.; Fouda, M. Crosslinking of Alginic Acid/Chitosan Matrices Using Polycarboxylic Acids and Their Utilization for Sodium Diclofenac Release. *Carbohydr. Polym.* **2008**, *73*, 606–611. [[CrossRef](#)]
31. Varshosaz, J.; Alinagari, R. Effect of Citric Acid as Cross-Linking Agent on Insulin Loaded Chitosan Microspheres. *Iran. Polym. J.* **2005**, *7*, 647–656.
32. Cui, Z.; Beach, E.; Anastas, P. Modification of Chitosan Films with Environmentally Benign Reagents for Increased Water Resistance. *Green Chem. Lett. Rev.* **2011**, *4*, 35–40. [[CrossRef](#)]
33. Salam, A.; Venditti, R.; Pawlak, J.; El-Tahlawy, K. Crosslinked Hemicellulose Citrate-Chitosan Aerogel Foams. *Carbohydr. Polym.* **2011**, *84*, 1221–1229. [[CrossRef](#)]
34. Olsson, E.; Hedenqvist, M.; Johansson, C.; Järnström, L. Influence of Citric Acid and Curing on Moisture Sorption, Diffusion and Permeability of Starch Films. *Carbohydr. Polym.* **2013**, *94*, 765–772. [[CrossRef](#)]
35. Reddy, N.; Yang, Y. Citric Acid Cross-Linking of Starch Films. *Food Chem.* **2010**, *118*, 702–711. [[CrossRef](#)]
36. Ritthidej, G.; Phaechamud, T.; Koizumi, T. Moist Heat Treatment on Physicochemical Change of Chitosan Salt Films. *Int. J. Pharm.* **2002**, *232*, 11–22. [[CrossRef](#)]
37. Tual, C.; Espuche, E.; Escoubes, M.; Domard, A. Transport Properties of Chitosan Membranes: Influence of Crosslinking. *J. Polym. Sci. Part B Polym. Phys.* **2000**, *38*, 1521–1529. [[CrossRef](#)]
38. Hsien, T.; Rorrer, G. Heterogeneous Cross-Linking of Chitosan Gel Beads: Kinetics, Modeling, and Influence on Cadmium Ion Adsorption Capacity. *Ind. Eng. Chem. Res.* **1997**, *36*, 3631–3638. [[CrossRef](#)]
39. Park, J.; Park, J.; Ruckenstein, E. Thermal and Dynamic Mechanical Analysis of PVA/MC Blend Hydrogels. *Polymer* **2001**, *42*, 4271–4280. [[CrossRef](#)]
40. Galiotta, G.; di Gioia, L.; Guilbert, S.; Cuq, B. Mechanical and Thermomechanical Properties of Films Based on Whey Proteins as Affected by Plasticizer and Crosslinking Agents. *J. Dairy Sci.* **1998**, *81*, 3123–3130. [[CrossRef](#)]
41. Demirgöz, D.; Elvira, C.; Mano, J.; Cunha, A.; Piskin, E.; Reis, R. Chemical Modification of Starch Based Biodegradable Polymeric Blends: Effects on Water Uptake, Degradation Behaviour and Mechanical Properties. *Polym. Degrad. Stab.* **2000**, *70*, 161–170. [[CrossRef](#)]
42. Silva, S.; Caridade, S.; Mano, J.; Reis, R. Effect of Crosslinking in Chitosan/Aloe Vera-Based Membranes for Biomedical Applications. *Carbohydr. Polym.* **2013**, *98*, 581–588. [[CrossRef](#)]
43. Casey, L.; Wilson, L. Investigation of Chitosan-PVA Composite Films and Their Adsorption Properties. *J. Geosci. Environ. Prot.* **2015**, *3*, 78–84. [[CrossRef](#)]
44. Roberts, G.; Taylor, K. The Formation of Gels by Reaction of Chitosan with Glutaraldehyde. *Macromol. Chem. Phys.* **1989**, *190*, 951–960. [[CrossRef](#)]
45. Pizzoli, M.; Ceccorulli, G.; Scandola, M. Molecular Motions of Chitosan in the Solid State. *Carbohydr. Polym.* **1991**, *222*, 205–213. [[CrossRef](#)]
46. Viciosa, M.; Dionisio, M.; Silva, R.; Reis, R.; Mano, J. Molecular Motions in Chitosan Studied by Dielectric Relaxation Spectroscopy. *Biomacromolecules* **2004**, *5*, 2073–2078. [[CrossRef](#)]
47. Nielsen, L.; Landel, R. *Mechanical Properties of Polymers and Composites*, 2nd ed.; Marcel Dekker, Inc.: New York, NY, USA, 1994.
48. Krongauz, V. Diffusion in Polymers Dependence on Crosslink Density. *J. Therm. Anal. Calorim.* **2010**, *102*, 435–445. [[CrossRef](#)]
49. Mitchell, J. The Rheology of Gels. *J. Texture Stud.* **1980**, *11*, 315–337. [[CrossRef](#)]

50. Gartner, C.; López, B.; Sierra, L.; Graf, R.; Spiess, H.; Gaborieau, M. Interplay between Structure and Dynamics in Chitosan Films Investigated with Solid-State NMR, Dynamic Mechanical Analysis, and X-ray Diffraction. *Biomacromolecules* **2011**, *12*, 1380–1386. [[CrossRef](#)]
51. Sakurai, K.; Takugi, M.; Takahashi, T. Crystal Structure of Chitosan. I. Unit Cell Parameters. *Sen'i Gakkaishi* **1984**, *40*, 246–253. [[CrossRef](#)]
52. Ferry, J. *Viscoelastic Properties of Polymers*, 3rd ed.; John Wiley & Sons Inc.: Hoboken, NJ, USA, 1980.
53. Mattei, G.; Ahluwalia, A. Sample, testing and analysis variables affecting liver mechanical properties: A review. *Acta Biomater.* **2016**, *45*, 60–71. [[CrossRef](#)] [[PubMed](#)]
54. Bartolini, L.; Iannuzzi, D.; Mattei, G. Comparison of frequency and strain-rate domain mechanical characterization. *Sci. Rep.* **2018**, *8*, 13697. [[CrossRef](#)] [[PubMed](#)]
55. Oyen, M.L. Nanoindentation of biological and biomimetic materials. *Exp. Technol.* **2013**, *37*, 73–87. [[CrossRef](#)]
56. van Hoorn, H.; Kurniawan, N.A.; Koenderink, G.H.; Iannuzzi, D. Local dynamic mechanical analysis for heterogeneous soft matter using ferrule-top indentation. *Soft Matter.* **2016**, *12*, 3066–3073. [[CrossRef](#)] [[PubMed](#)]
57. Lim, L.; Khor, E.; Ling, C. Effects of Dry Heat and Saturated Steam on the Physical Properties of Chitosan. *J. Biomed. Mater. Res.* **1999**, *48*, 111–116. [[CrossRef](#)]
58. Neto, C.; Giacometti, J.; Job, A.; Ferreira, F.; Fonseca, J. Thermal Analysis of Chitosan Based Networks. *Carbohydr. Polym.* **2005**, *62*, 97–103. [[CrossRef](#)]
59. Correia, D.; Gámiz-González, M.; Botelho, G.; Vidaurre, A.; Gomez Ribelles, J.; Lanceros-Mendez, A.; Sencadas, V. Effect of Neutralization and Cross-Linking on the Thermal Degradation of Chitosan Electrospun Membranes. *J. Therm. Anal. Calorim.* **2014**, *117*, 123–130. [[CrossRef](#)]
60. Sakurai, K.; Maegawa, T.; Takahashi, T. Glass Transition Temperature of Chitosan and Miscibility of Chitosan/Poly(N-Vinyl Pyrrolidone) Blends. *Polymer* **2000**, *41*, 7051–7056. [[CrossRef](#)]



© 2019 by the authors. Licensee MDPI, Basel, Switzerland. This article is an open access article distributed under the terms and conditions of the Creative Commons Attribution (CC BY) license (<http://creativecommons.org/licenses/by/4.0/>).